Supplemental Information

The Schlemm's canal is a VEGF-C/VEGFR-3 responsive lymphatic-like vessel

Aleksanteri Aspelund, Tuomas Tammela, Salli Antila, Harri Nurmi, Veli-Matti Leppänen, Georgia Zarkada, Lukas Stanczuk, Mathias Francois, Taija Mäkinen, Pipsa Saharinen, Ilkka Immonen, Kari Alitalo

Supplemental Figure 1-13

Supplemental Video 1-5 Legends

Supplemental Results

Supplemental Methods

Supplemental References

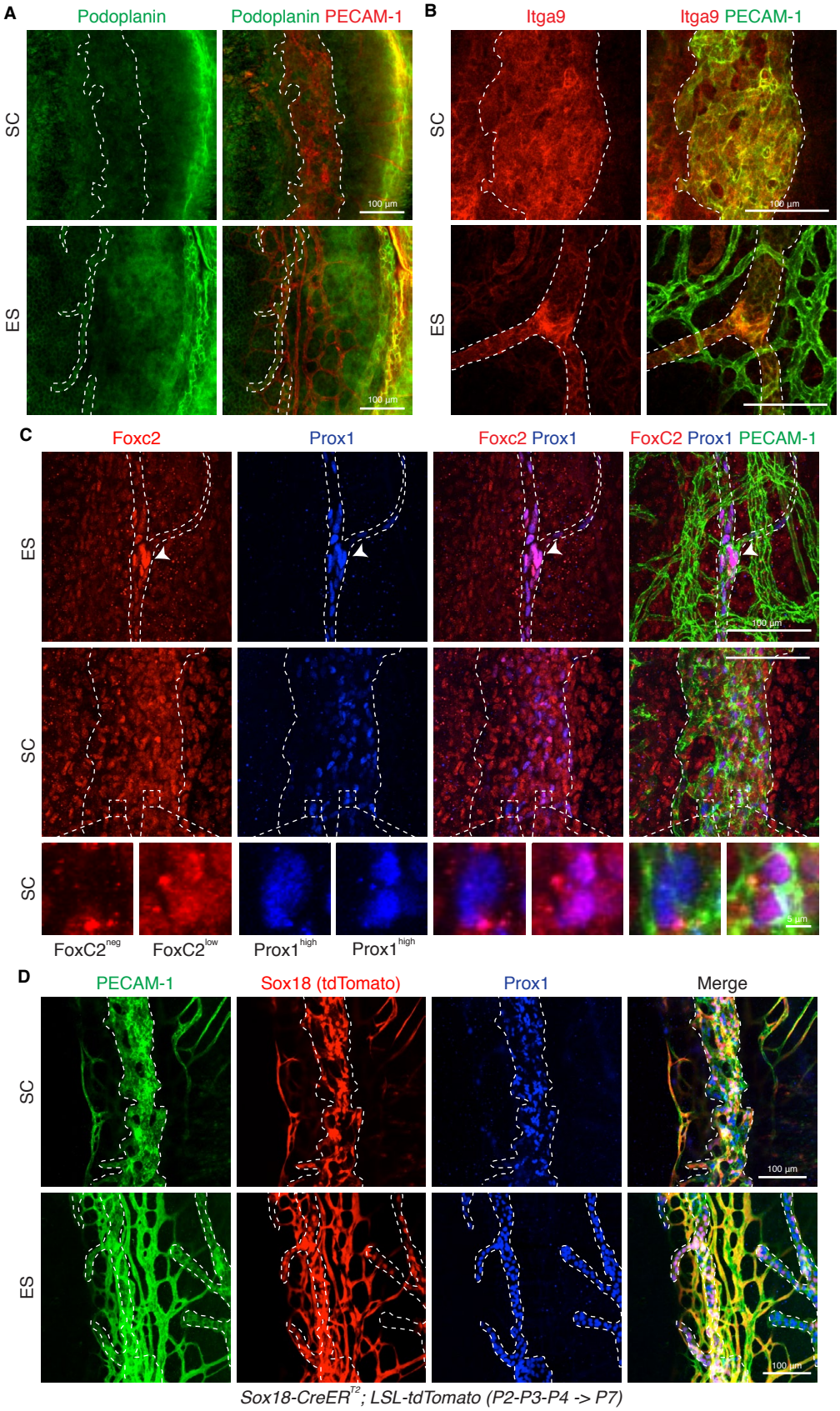

Supplemental Figure 1

SC ECs display Itga9 and Foxc2 expression, Sox18-CreER^{T2} activity at P2-P4, but lack podoplanin expression. **(A-C)** Immunostaining of podoplanin, Itga9 and Foxc2 expression by SC ECs and ES lymphatic vessels (both indicated by *dashed line*). (C) *Insets* show the heterogenous Foxc2 expression pattern by SC ECs. Note FoxC2^{low} and FoxC2^{neg} Prox1^{pos} SC ECs. Lymphatic valve indicated by *arrowhead*. (**D**) Visualization of Sox18 lineage tracing activity in SC ECs in *Sox18-CreER^{T2}; LSL-tdTomato* lineage tracer mice after injection of 4-OHT at P2, P3 and P4, with analysis at P7. Scale bars: 100 µm (A-D), 5 µm (D *inset*).

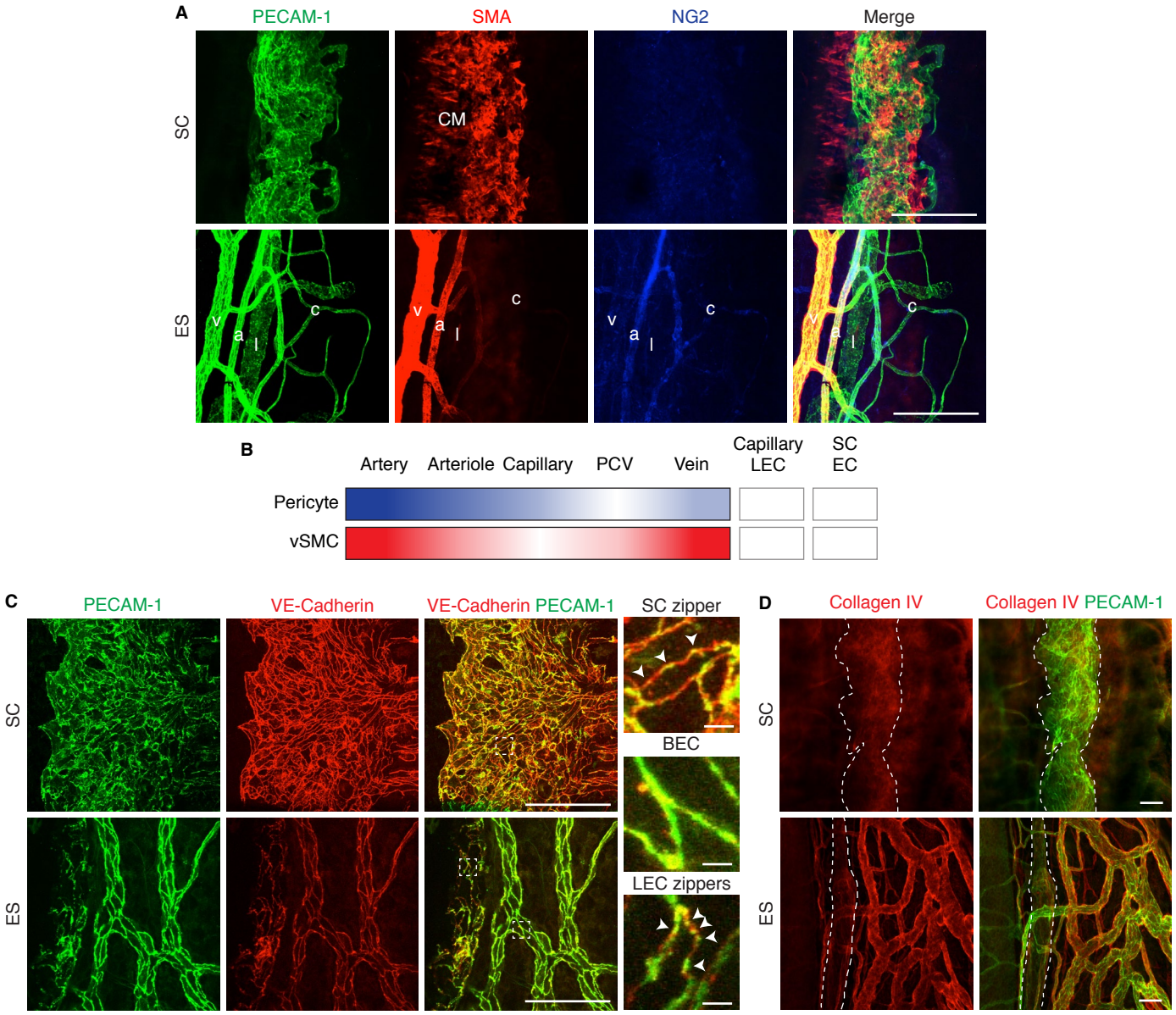

Supplemental Figure 2
SC lacks pericytes and vascular smooth muscle cells, but has basement membrane collagen IV and zipper-type EC junctions. (A) Immunofluorescence staining of PECAM-1, SMA and NG2 in adult mice. *CM* ciliary muscle. (**B**) PCs and vSMC staining in arteries (*a*), arterioles, capillaries (*c*), postcapillary venules (*pcv*), veins (*v*), lymphatic capillaries (*c*) and SC in the anterior eye. (**C**) Staining of EC junctions in the SC using antibodies against VE-Cadherin and PECAM-1. Note zipper-type VE-Cadherin staining but spotwise PECAM-1 staining is observed in SC ECs and in LECs (*insets*). (**D**) Staining of collagen IV around SC ECs and LECs (both indicated by *dashed line*). Scale bars: 100 µm (A, C), 50 µm (D) and 5 µm (*inset* in C).

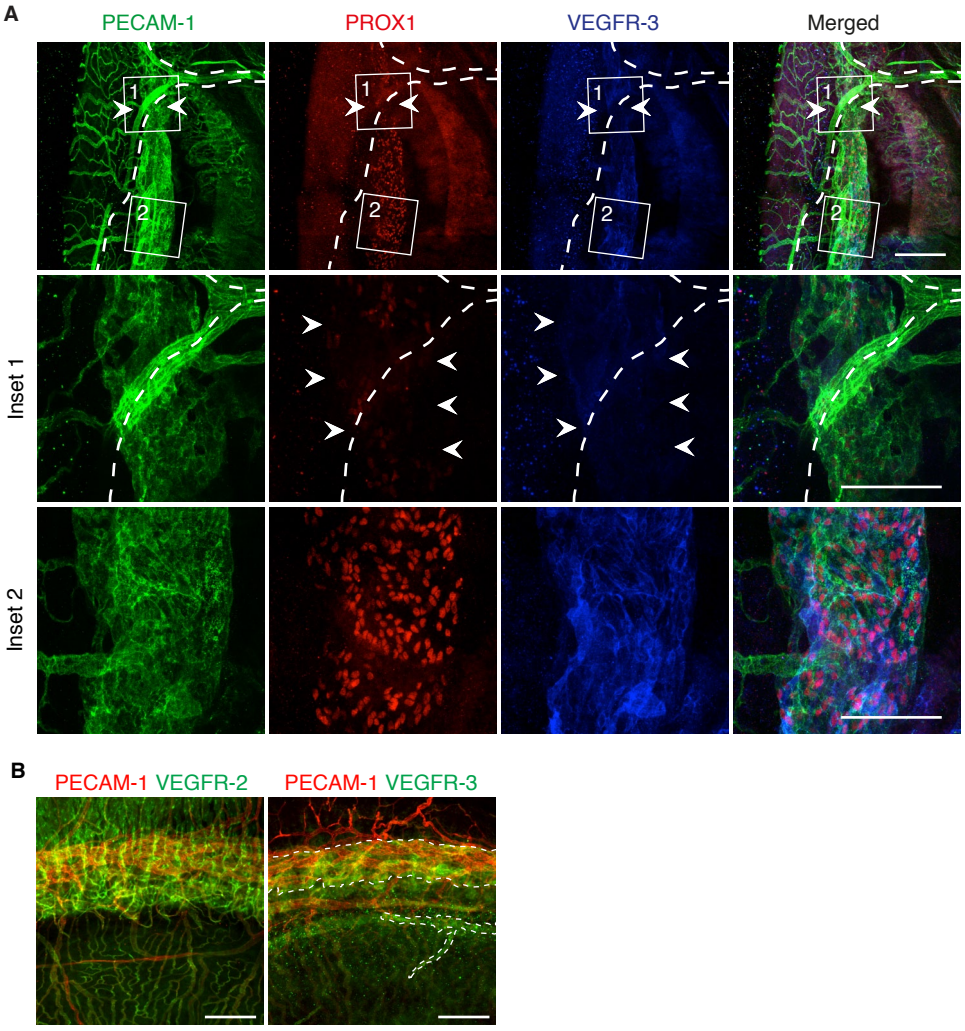

Supplemental Figure 3
Downregulation of Prox1 and VEGFR-3 in SC endothelium in proximity of the long posterior ciliary artery and VEGFR-2/3 expression pattern. (A) The SC and the long posterior ciliary artery (indicated by *dashed line*) were visualized by immunofluorescence staining in adult mice. *Inset 1* shows SC in proximity of the long posterior ciliary artery and *inset 2* shows normal SC endothelium. VEGFR-3 and Prox1 downregulated areas are indicated by the *arrowhead*. (**B**) Visualization of VEGFR-2 and VEGFR-3 expression in the limbus by immunofluorescence staining. Scale bars: 200 µm.

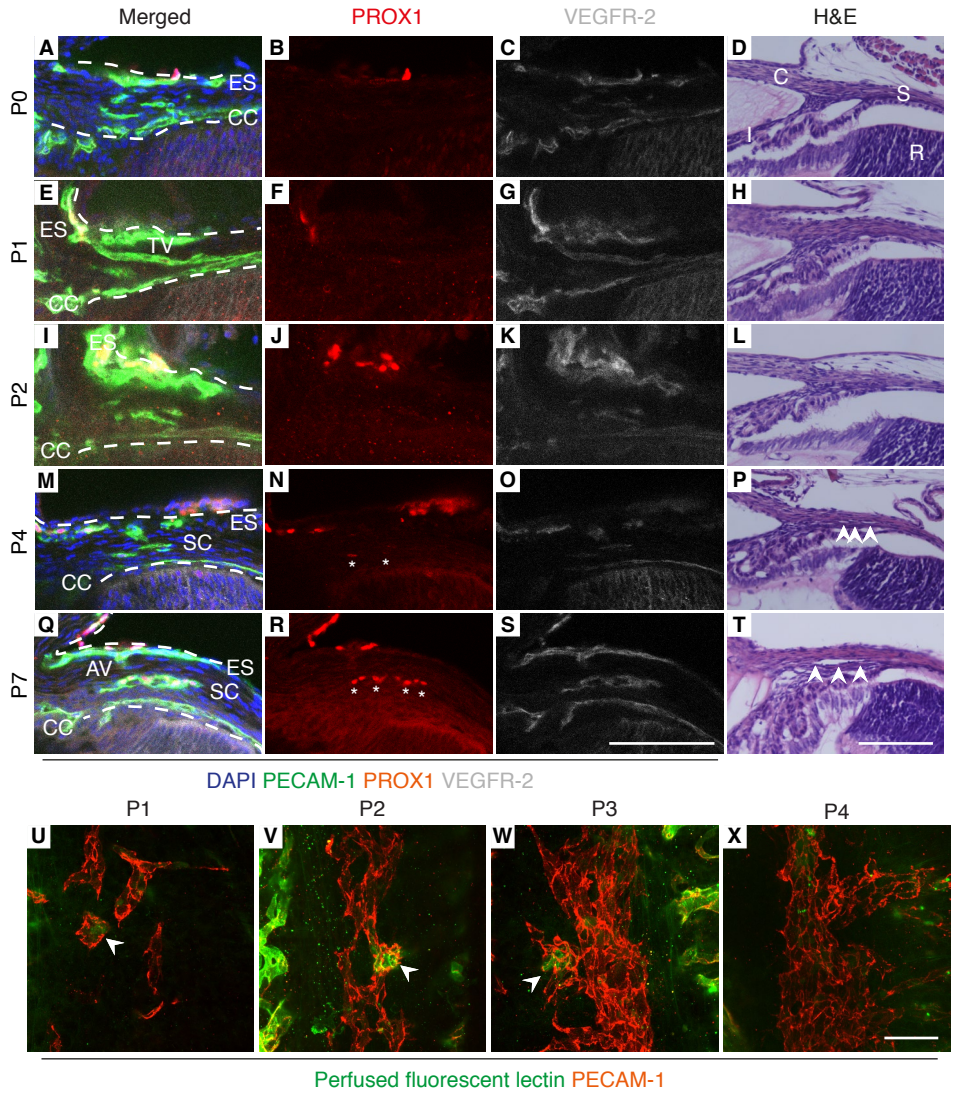

Supplemental Figure 4

The SC develops from transscleral veins and becomes blind-ended postnatally. (A-T) Representative images of the developing SC (indicated by the *dashed line*) at P0, P1, P2, P4 and P7 as visualized by immunofluorescence staining in thick sections, and in H&E stained sections. *ES*, episclera. *CC*, choriocapillaries. *SC*, Schlemm's canal. *TV*, transscleral vessel. *S*, sclera. *R*, retina. *I*, iris. * indicates Prox1 expression. (**U-X**) Representative images of the developing SC at P1, P2, P3 and P4 visualized by whole mount immunofluorescence staining in fluorescent lectin perfused pups. *Arrowhead* indicates lectin perfusion through transscleral vein. Note the absence of perfused transscleral veins at P4. Scale bars, 100 µm.

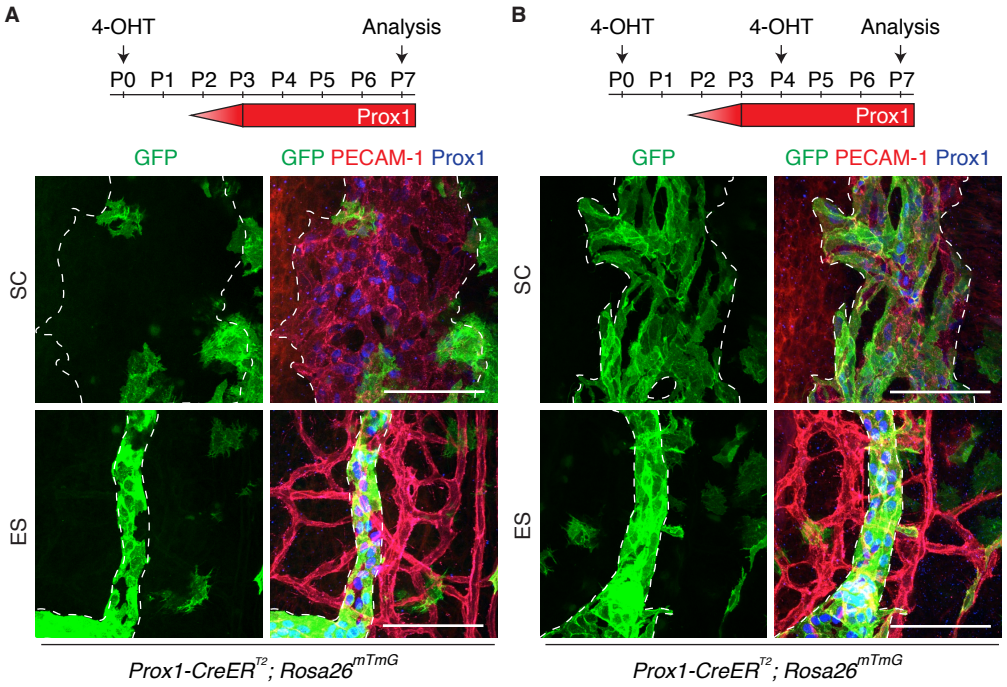

Supplemental Figure 5
SC ECs do not originate from pre-existing LECs. Representative images of the SC and ES lymphatics (both indicated by the *dashed line*) at P7 after injection of 4-OHT at P0 (**A**) or P0 and P4 (**B**). The limbal vasculature is stained in whole mount with antibodies against PECAM-1 (green) and Prox1 (blue). Scale bars, 100 µm.

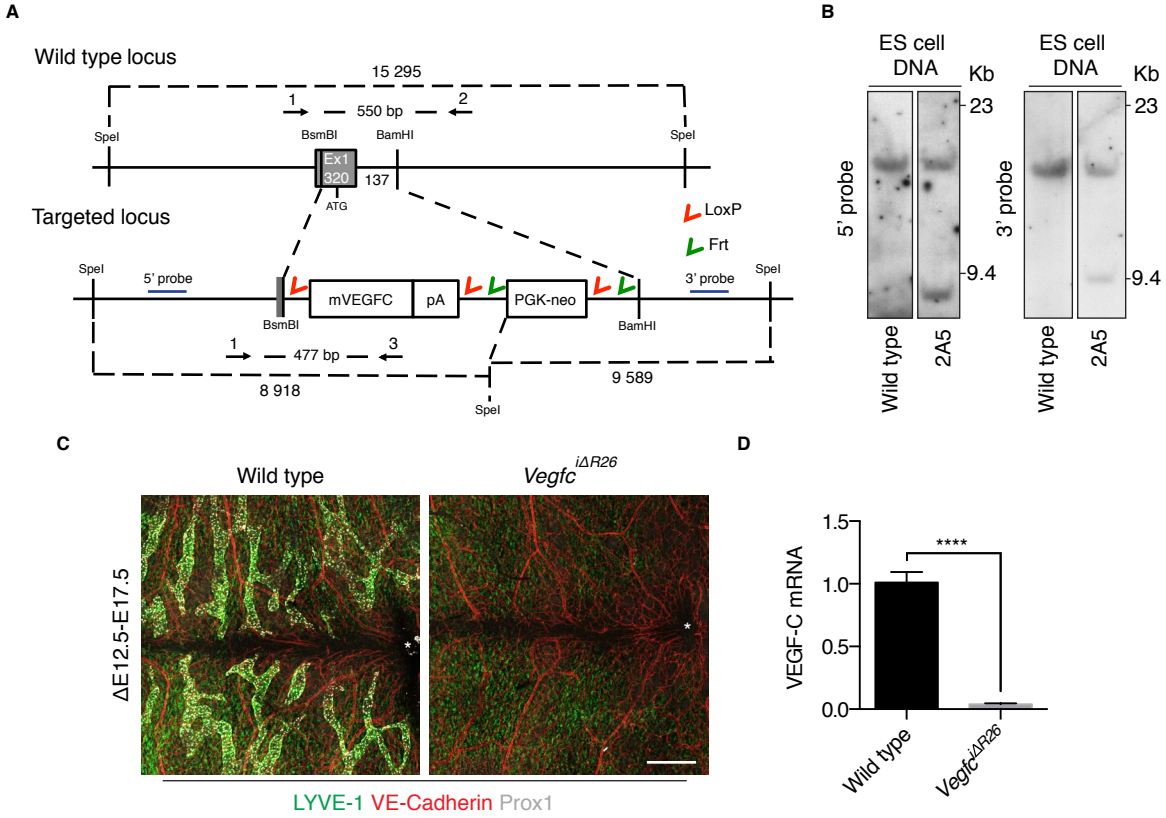

Supplemental Figure 6

Conditional targeting of the *Vegfc* locus. (**A**) The homologous recombination event deletes 137 bp of genomic DNA sequences at the beginning of the 1st intron, via insertion of a mouse Vegfc cDNA-bovine growth hormone polyA signal and a neomycin cassette flanked by loxP and Frt sites. Red arrowheads, *loxP* sites; green arrowheads, FRT sites; 1, 2 and 3, primers used for PCR genotyping; external 5' and 3' hybridization probes are indicated. (**B**) Southern blot analysis of SpeI digested ES cell DNA. λHindIII molecular marker is shown on the right. (**C**) Whole mount immunohistochemical staining of the ventral skin in *Vegfc*$^{i\Delta R26}$ and control littermates with indicated antibodies. After administration of 4-OHT at E12.5 and E13.5, and analysis at E18.5, *Vegfc*$^{i\Delta R26}$ embryos were characterized by aplasia of cutaneous lymphatic vasculature. *, umbilical area. $n > 4$ embryos/genotype. (**D**) VEGF-C mRNA RT-qPCR of P5 lung lysates after daily 4-OHT administration from P1 to P4. Scale bars: 300 μm.

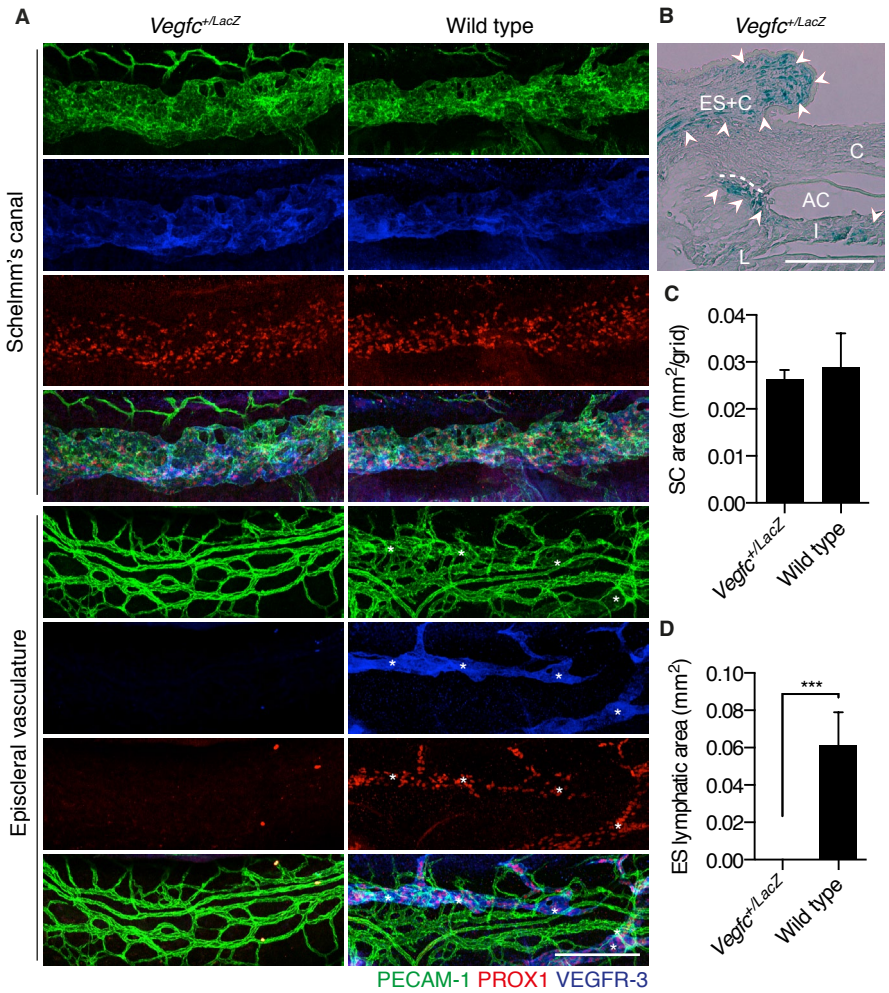

Supplemental Figure 7

Normal SC morphogneesis in *Vegfc* haploinsufficient mice at P12. (**A**) Immunofluoresence staining of *Vegfc*$^{+/LacZ}$ and wild type littermate SC and ES lymphatics of using antibodies against PECAM-1 (green), Prox1 (red) and VEGFR-3 (blue). ES lymphatics are indicated by *. (**B**) VEGF-C expression (indicated by *arrowheads*) detected by X-gal staining in *Vegfc*$^{+/LacZ}$ reporter mice. SC is indicated by dashed line. *I*, Iris. *C*, Cornea. *AC*, anterior chamber. *ES+C*, episclera and conjunctiva. Quantitative analysis of the PECAM-1-positive SC area (**C**) and VEGFR-3 and Prox1-positive ES lymphatic (**D**) area in *Vegfc*$^{+/LacZ}$ and wild type (WT) littermate mice. *n* = 4 per genotype. Scale bars, 200 µm (A); 50 µm (B).

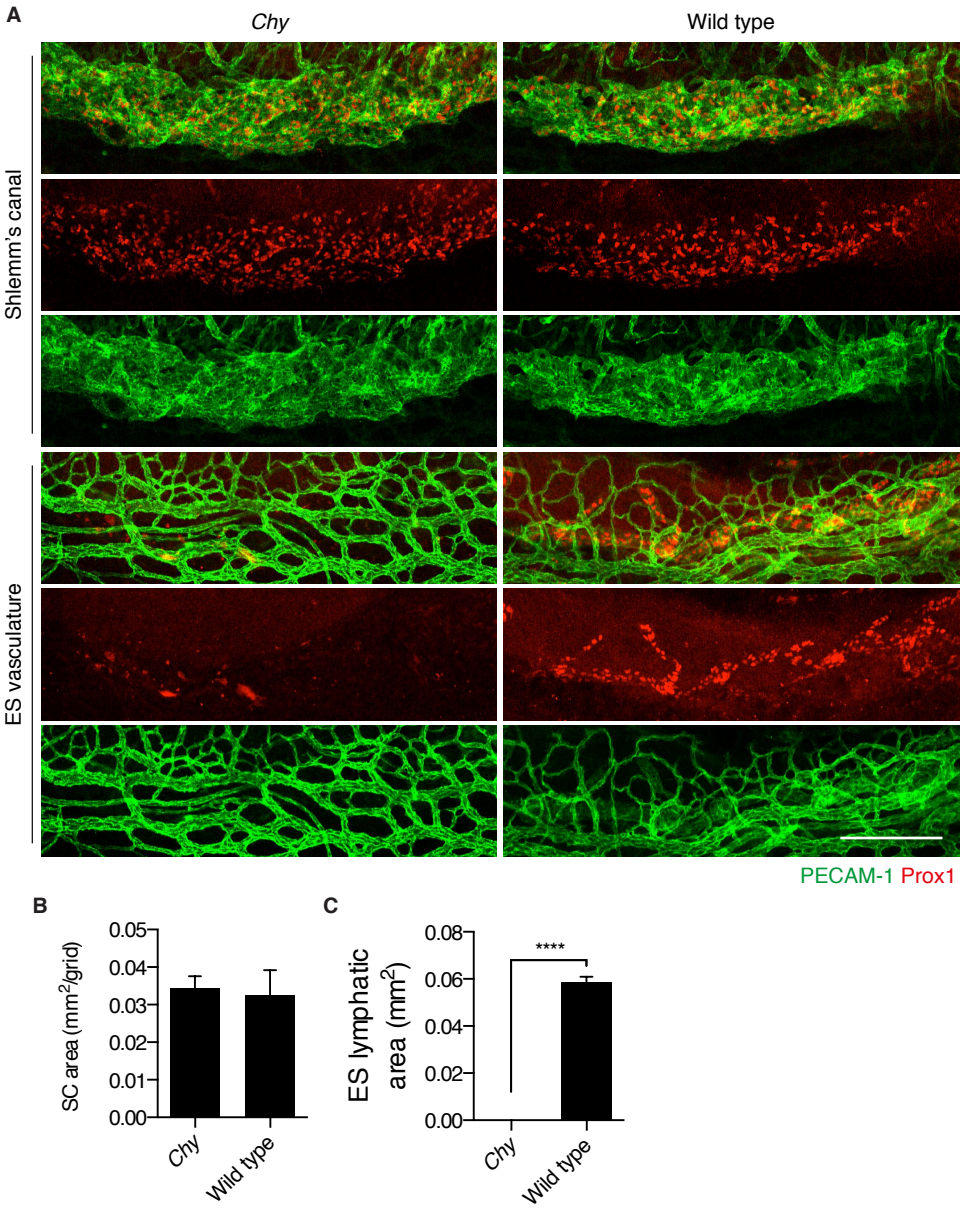

Supplemental Figure 8
Normal SC morphogenesis in *Chy* mice at P12. (**A**) Immunofluorescence staining of the murine SC and ES vasculature around the limbus in *Chy* (n = 4) and wild type littermates (WT, n = 4) mice using antibodies against PECAM-1 (green) and Prox1 (red). Quantification of the PECAM-1-positive SC surface area (**B**) and the PECAM-1 and Prox1-positive ES lymphatic surface area (**C**) shown in (a**)**. Scale bars, 200 µm.

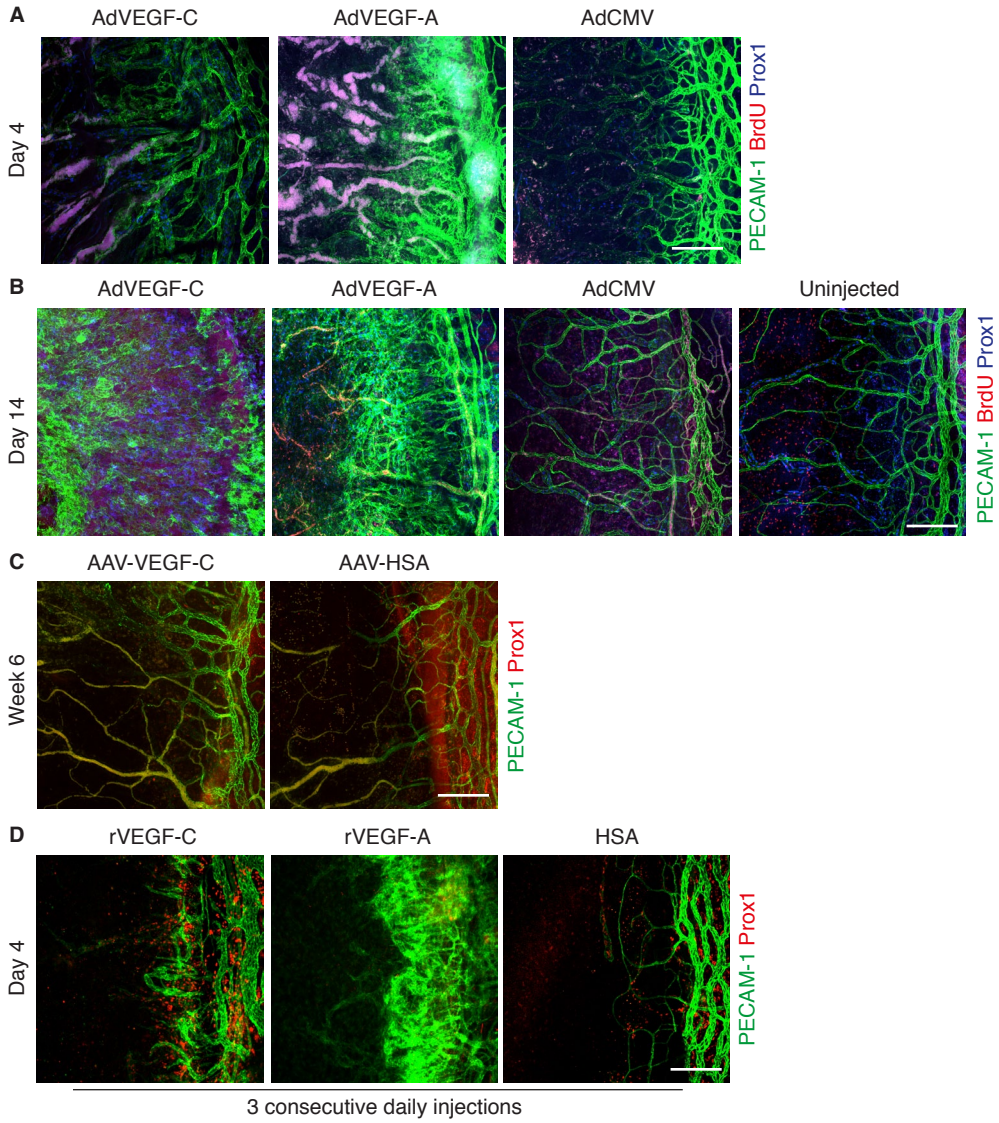

Supplemental Figure 9

Corneal neovascularization in VEGF-C and VEGF-A injected eyes. (A-B) Immunofluorescence staining of the corneal vasculature around the limbus in AdVEGF-C, AdVEGF-A and AdControl injected eyes, and in uninjected eyes using antibodies against PECAM-1 (green), BrdU (red) and Prox1 (blue) at 4 days and 14 days after injection. Prior to sacrifice, the mice received on injection of 100 mg/kg of BrdU to label proliferating cells. (**C**) Immunofluorescence staining of the corneal vasculature around the limbus 6 weeks after injection of AAV-VEGF-C and AAV-HSA using antibodies against PECAM-1 (green) and Prox1 (red). (**D**) Staining on day 4 after three consecutive daily injections of rVEGF-C, rVEGF-A or HSA using antibodies against PECAM-1 (green) and Prox1 (red). Scale bars, 200 µm (A-D).

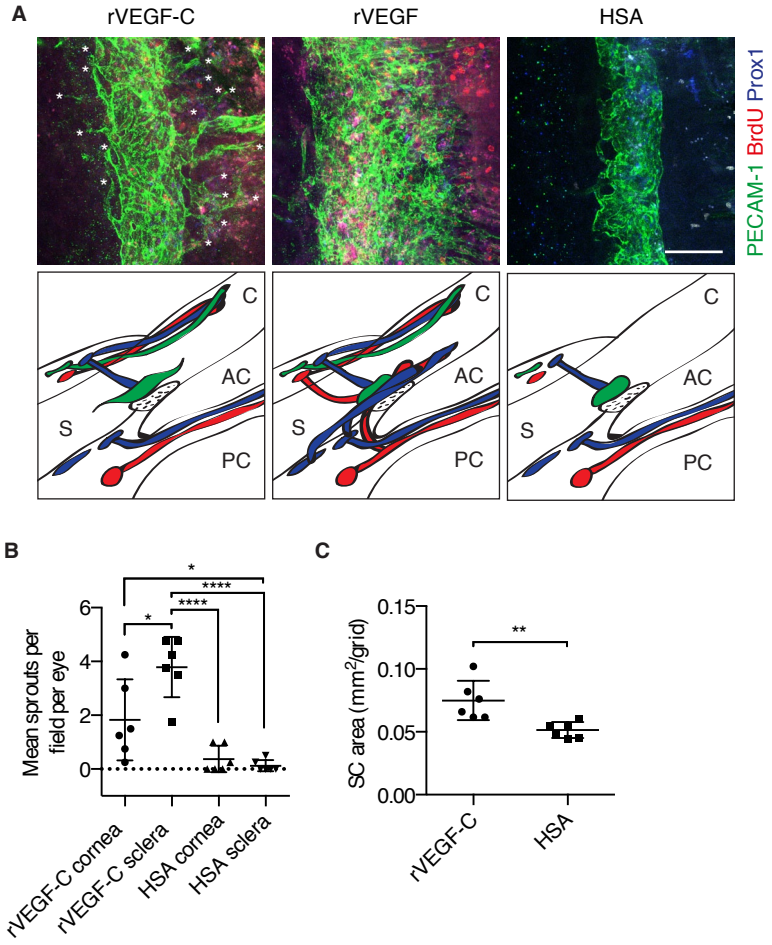

Supplemental Figure 10
Three daily consecutive injections of recombinant VEGF-C induce sprouting of SC ECs and growth of the SC. Analysis of changes in SC morphology on day 4 after injection of 3.8 μg recombinant rVEGF-C, rVEGF or HSA into the anterior chamber on three consecutive days. To identify proliferating ECs, the mice were injected with 100 mg/kg BrdU 2h prior to sacrifice. (**A**) Immunofluorescence staining of the SC with antibodies against PECAM-1 (green), BrdU (red) and Prox1 (blue) and illustration of the changes in limbal vascular anatomy after injections. *Asterisks* denotes sprouts of the SC ECs. (**B-C**) Quantitative analysis of mean SC EC sprouts per field per eye toward the cornea or the sclera and SC area. Each dot represents data from one eye. The SC was not quantified in rVEGF-injected eyes, as it could not be distinguished. Scale bars, 100 µm.

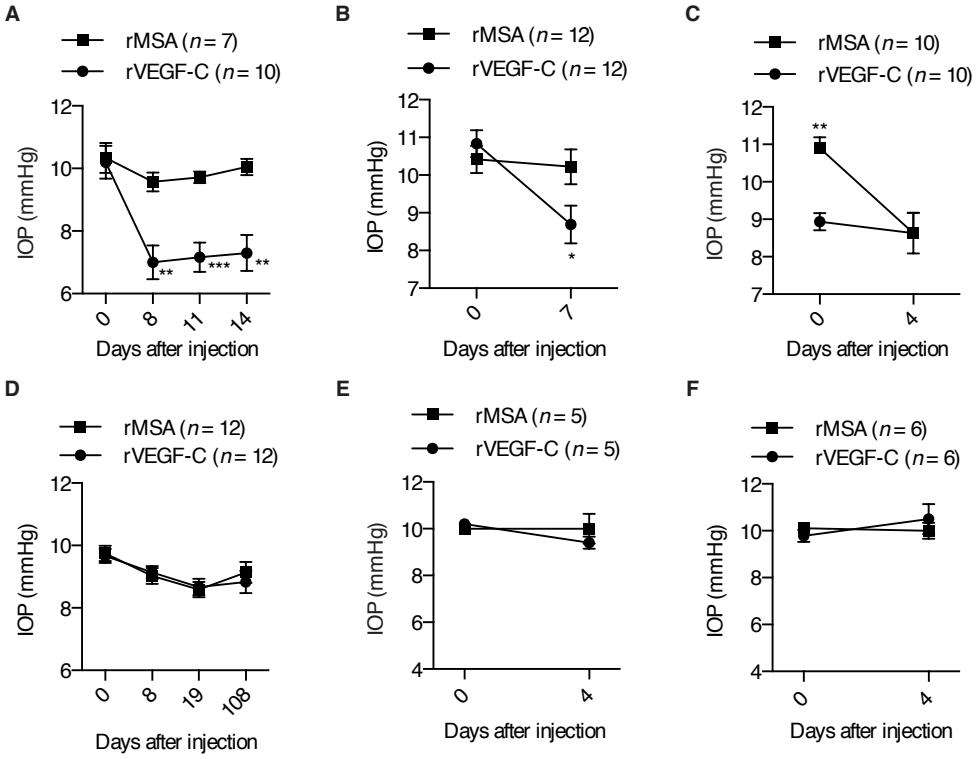

Supplemental Figure 11

Effects of a single injection of rVEGF-C on IOP. (**A-F**) Analysis of changes in IOP after injection of recombinant VEGF-C (rVEGF-C), or mouse serum albumin (rMSA) into the anterior chamber of age-controlled female mice. Female age-controlled 35-36 week NMRI (A-C), 15 week NMRI (D) and 25 week Albino B6 (E-F) mice were used. 0.264 µg (B), 3.8 µg (A), 6.4 µg (C, E), 9.6 µg (F) of protein was injected in 4 µl. *n*-number are indicated in the figures. A significant proportion of the injected fluid was backflushed.

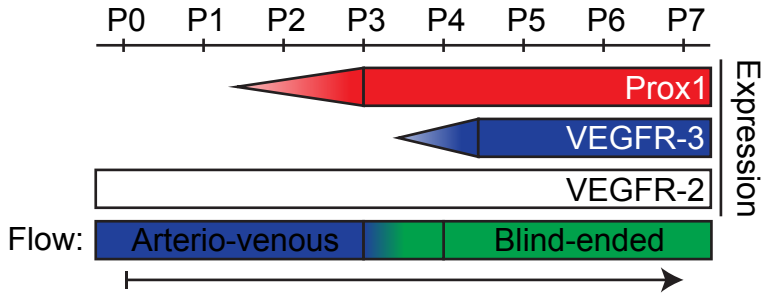

Supplemental Figure 12
Schematic of the SC developmental timeline. Induction of Prox1 by P2, induction of VEGFR-3 by P4 and expression of VEGFR-2 thorough all developmental stages of SC development. Transition from arteriovenous into blind-ended lymphatic-like vessel at P3-P4.

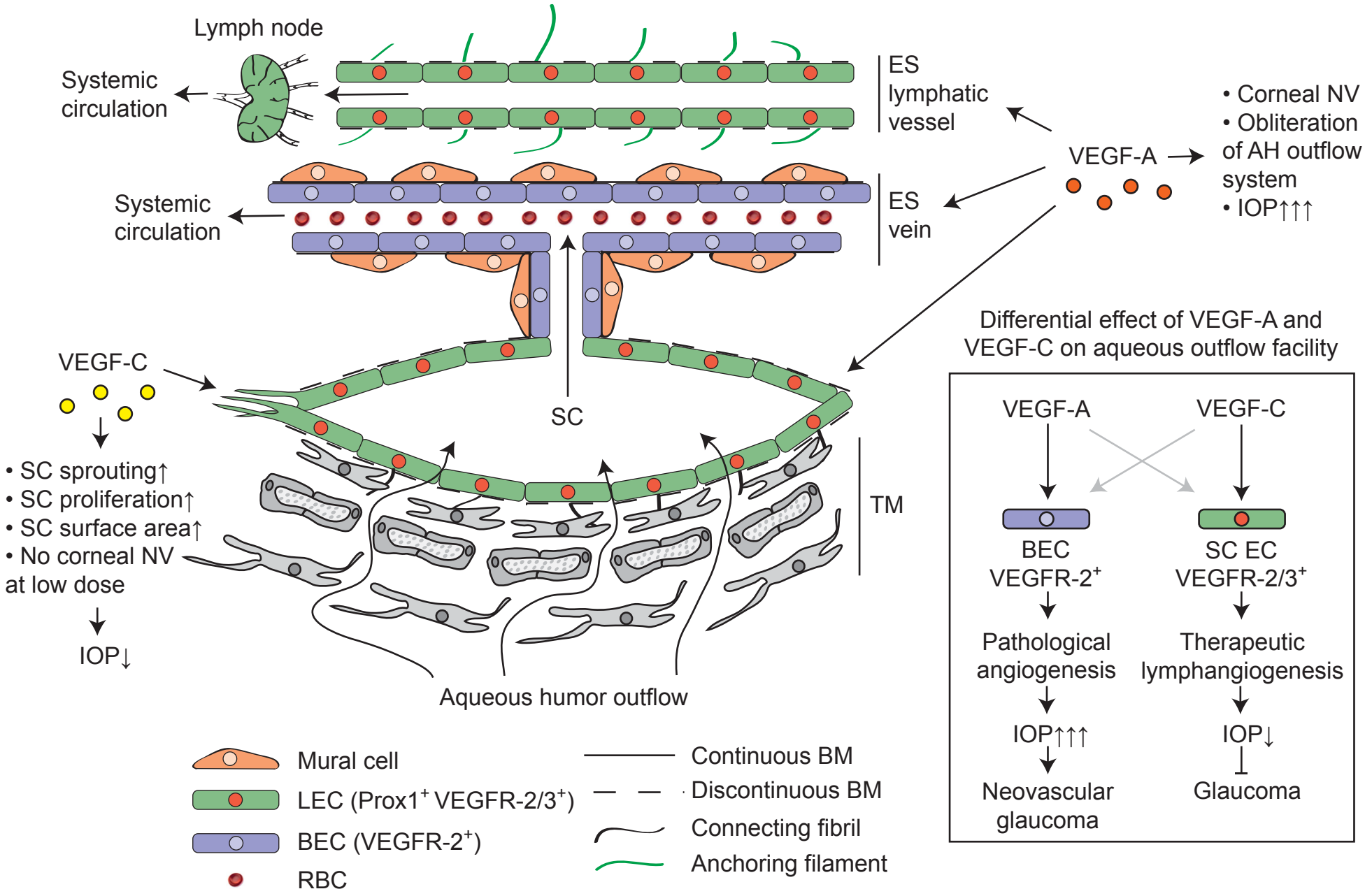

Supplemental Figure 13
Schematic model of the differential effects of VEGF and VEGF-C on the aqueous outflow system. VEGF and VEGF-C have dramatically different effects on the vascular aqueous outflow system. VEGFR-3 expression is restricted to SC ECs and ES LECs. VEGFR-2 expression is detected in all BECs, including choriocapillaries, blood vessels of the iris, ES blood vessels, and in LECs. VEGF-A affects all ECs, induces obliteration of the aqueous outflow system and massively increases IOP. VEGF-C effects are preferentially restricted to SC ECs and LECs, although it can be cleaved to activate VEGFR-2 in blood vessels (1). VEGF-C preferentially induces the growth of the SC. Even with massive VEGF-C overexpression, which induces the formation of a sheet-like SC in the cornea, a trend toward IOP reduction is observed. With small enough doses, corneal neovascularization can be avoided, but effects on the SC are sustained. Injection of rVEGF-C is associated with a sustained decrease in IOP.

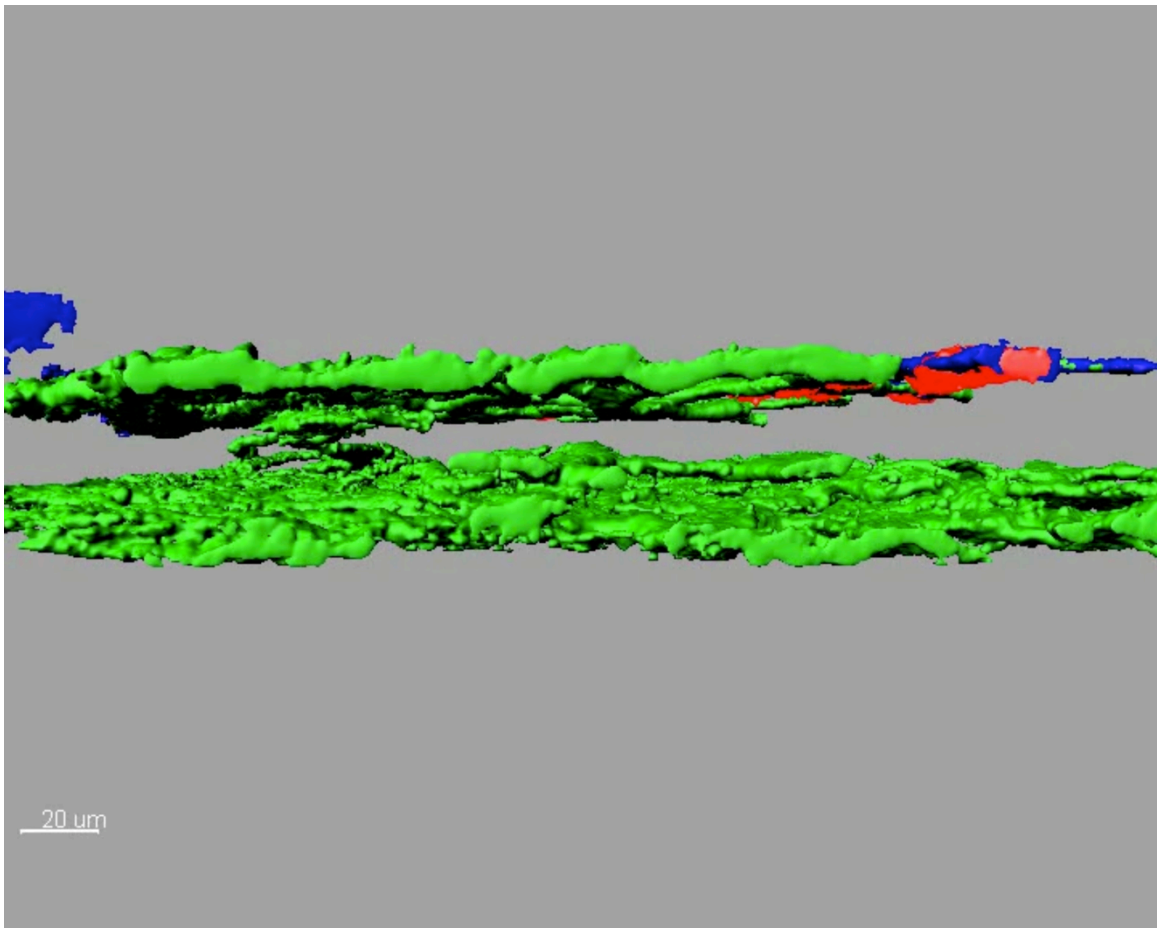

Supplemental Video 1. The developing SC at P0. Three-dimensional reconstruction of the confocal stack shown in Fig. 2A-C. The green, red and blue volume renderings are representative of the immunofluorescence for PECAM-1, Prox1 and VEGFR-3, respectively. The upper vascular layers of the video represent the ES vasculature with blood vessels in green and a lymphatic vessel in blue and red. The lower layer represents the choroidal layer with CCs in green. These two layers are connected by a network of transcleral vessels. Extensions from the CCs extending toward the ES layer are also seen.

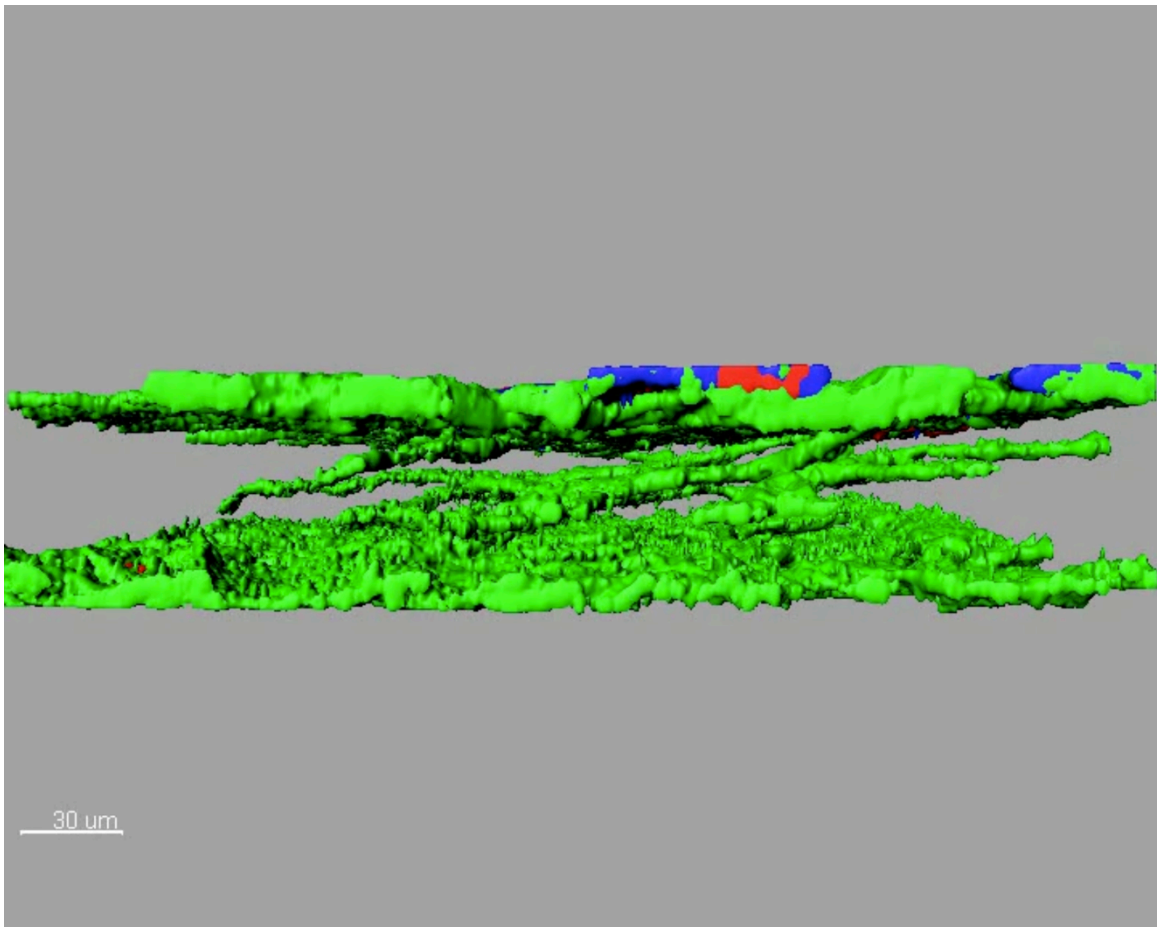

Supplemental Video 2. The developing SC at P1. Three-dimensional reconstruction of the confocal stack shown in Fig. 2D-F. The green, red and blue volume renderings are representative of the immunofluorescence for PECAM-1, Prox1 and VEGFR-3, respectively. The upper vascular layers of the video represent the ES vasculature with blood vessels in green and a lymphatic vessel in blue and red. The lower layer represents the choroidal layer with CCs in green. These two layers are connected by a network of transcleral vessels. Note that the transcleral vessels appear to send strings of ECs toward adjacent transscleral vessels.

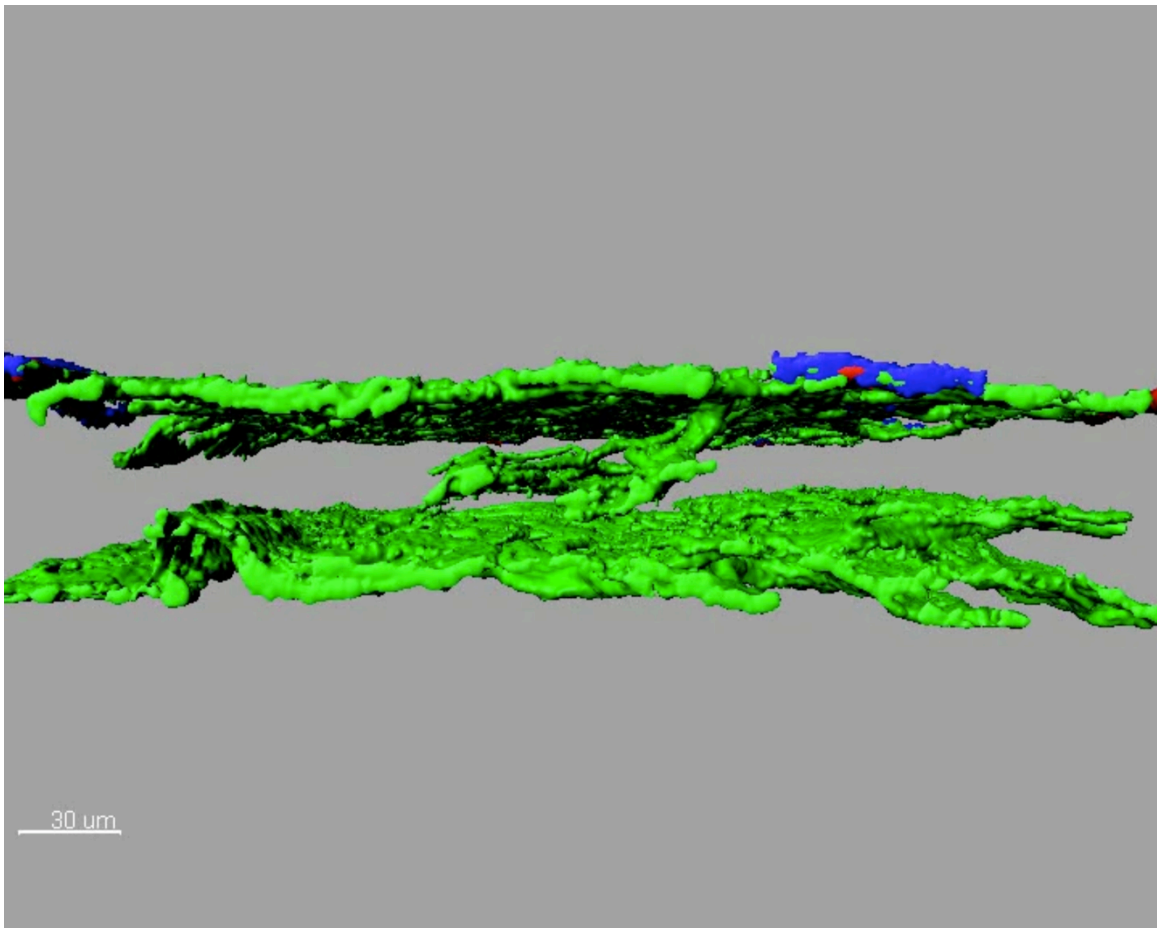

Supplemental Video 3. The developing SC at P2. Three-dimensional reconstruction of the confocal stack shown in Fig. 2G-I. The green, red and blue volume renderings are representative of the immunofluorescence for PECAM-1, Prox1 and VEGFR-3, respectively. The upper vascular layers of the video represent the ES vasculature with blood vessels in green and a lymphatic vessel in blue and red. The lower layer represents the choroidal layer with CCs in green. The strings of ECs between adjacent transscleral vessels have started to coalesce into a rudimentary SC. Prox1 expression is detected at sites furthest away from the two long posterior ciliary arteries.

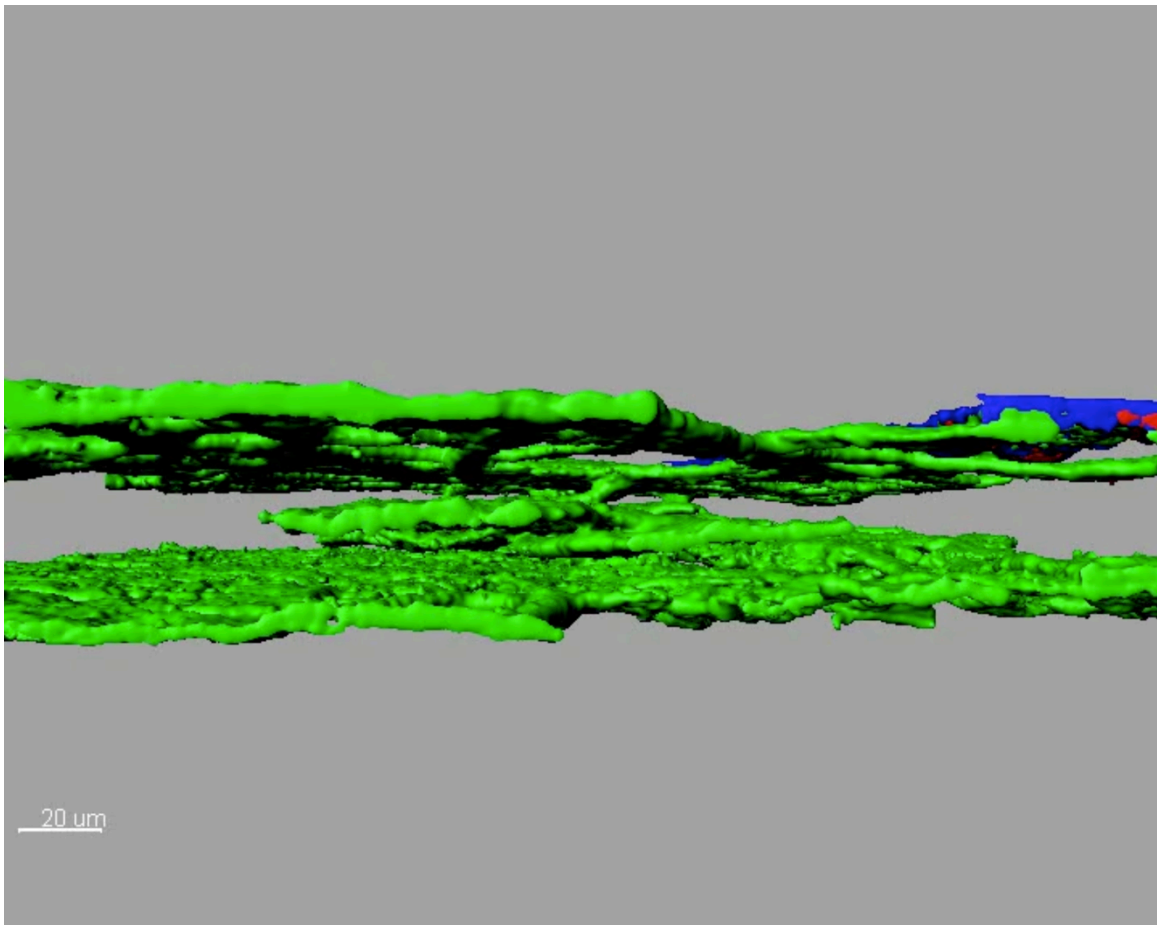

Supplemental Video 4. The developing SC at P4. Three-dimensional reconstruction of the confocal stack shown in Fig. 2J-L. The green, red and blue volume renderings are representative of the immunofluorescence for PECAM-1, Prox1 and VEGFR-3, respectively. The upper vascular layers of the video represent the ES vasculature with blood vessels in green and a lymphatic vessel in blue and red. The lower layer represents the choroidal layer with CCs in green. The SC has matured and luminalized. Prox1 expression is detected throughout the canal. Phantoms of a connection between the SC and CCs are observed. Very low VEGFR-3 expression is detected in the SC.

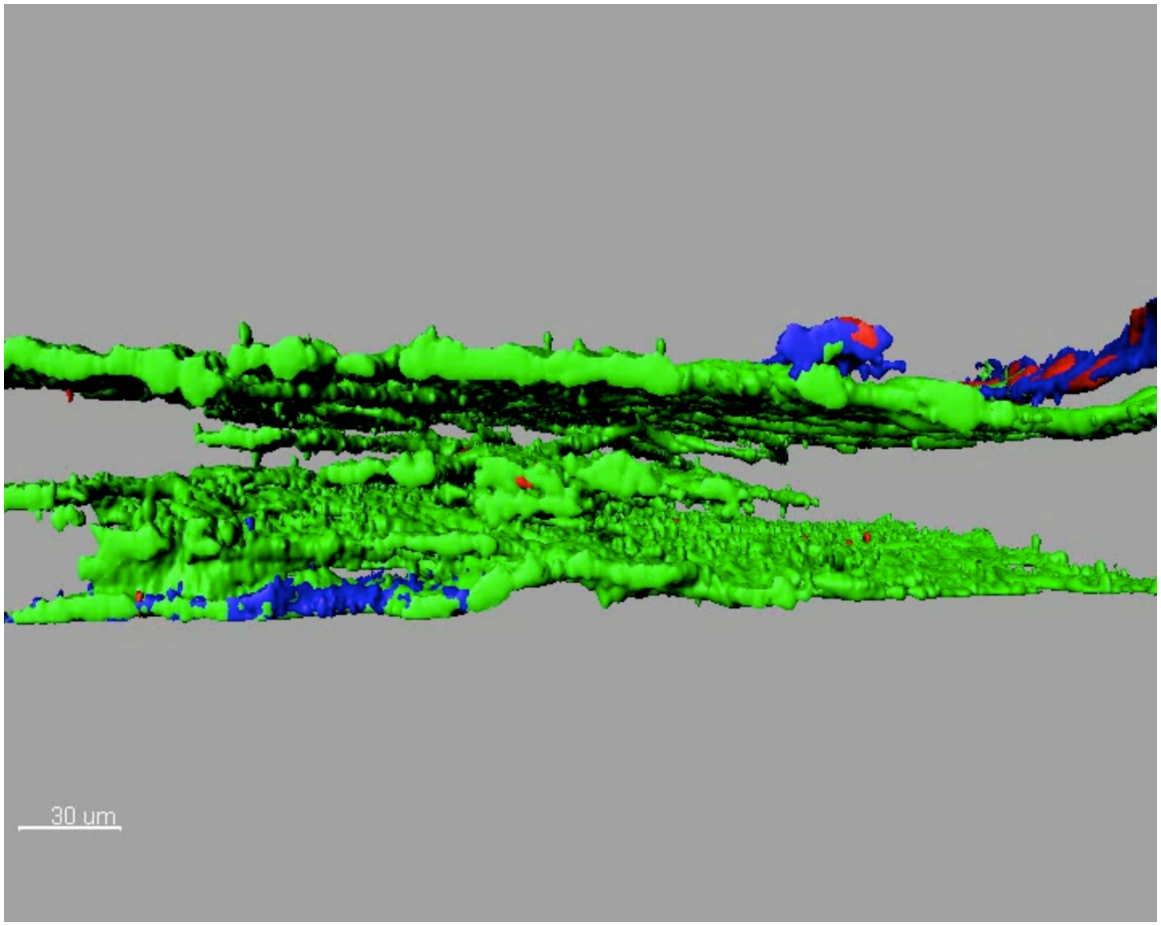

Supplemental Video 5. The developing SC at P7. Three-dimensional reconstruction of the confocal stack shown in Fig. 2M-O. The green, red and blue volume renderings are representative of the immunofluorescence for PECAM-1, Prox1 and VEGFR-3, respectively. The upper vascular layers of the video represent the ES vasculature with blood vessels in green and a lymphatic vessel in blue and red. The lower layer represents the choroidal layer with CCs in green. The SC has further matured and grown in size. Prox1 and VEGFR-3 expression is detected throughout the SC.

Supplemental Results

Downregulation of Prox1 and VEGFR-3 in proximity to the long posterior ciliary artery. Whole mount staining of the SC revealed significant Prox1 and VEGFR-3 downregulation in the proximity of the long posterior ciliary arteries, which are the two major choroidal arteries that cross the SC posteriorly to supply the iris. In these areas, only high magnification imaging revealed very low levels of Prox1 and VEGFR-3 expression and the corresponding SC area appeared narrow and hypoplastic, containing holes and breaks in the endothelium (**Supplemental Fig. 1**).

The SC becomes blind-ended between P3 and P4. Ocular immune privilege is achieved via several strategies that prevent or modify innate and adaptive immune responses in the eyes. Importantly, the inner eye is separated by the blood-eye barrier (2). Access of systemically delivered antibodies may be limited by the development of the blood-eye barrier. To determine the exact time of the transition into a blind-ended tube, fluorescent lectin was injected through the heart into newborn pups, and allowed to circulate for 5 minutes prior to sacrifice. In whole mount imaging of the PECAM-1 stained, lectin perfused eyes, transscleral vessels were still observed at P3, but no longer at P4 (**Supplemental Fig. 2U-X**), indicating that the SC becomes a blind-ended tube between P3 and P4 when VEGFR-3 expression is induced. These results indicate that antibody access to block VEGFR-3 on SC ECs may be compromised.

AAV-VEGF-C and AdVEGF-C aggravate baseline corneal neovascularization in *nu/nu* mice and high amounts of rVEGF-C activate ES blood vessels. Although abnormal corneal vasculature was detected in uninjected NMRI *nu/nu* mice, aggravation

corneal neovascularization was observed in both AdVEGF and AdVEGF-C injected eyes (**Supplemental Fig. 8A,B**), and in AAV-VEGF-C injected eyes (**Supplemental Fig. 5C**). No corneal neovascularization was detected at baseline in NMRI mice, but three injections of 3.8 μg of rVEGF-C on three consecutive days induced activation of ES blood vessels, but no corneal neovascularization (**Supplementary Fig. 8D**). Blood vessels extending toward the cornea were detected in rVEGF-injected eyes (Supplementary Fig. 8D).

Supplemental Methods

Generation of *Vegfc* gene targeted mice

The *Vegfc* region was isolated from a 129Sv mouse genomic library (3). A SpeI-AflII DNA fragment containing the 3.3-kilobase (kb) 5′ arm was cloned into the BamHI site of the p3ARM-KT vector. A 2.9-kilobase BamHI–PstI 3′ arm fragment was cloned into the *BglII-NsiI* sites of the p3ARM-KT vector. A KpnI-HindIII fragment from p3ARM-KT, containing both the 5' and 3' arms surrounding a NotI-AscIII unique cloning site, was transferred into pKOF-TK vector containing the thymidine kinase gene. The PGK-Neo cassette flanked by LoxP and Frt sites, as indicated in the Fig. S1, was cloned as an EcoRI-KpnI fragment into pBluescript.

Mouse Vegfc cDNA was PCR amplified and cloned into pBluescript. A genomic DNA fragment containing the polyA signal of the bovine growth hormone gene was PCR amplified and cloned as a XbaI fragment into the NheI site, located 3' of the mVegfc cDNA. The Vegfc-BGH-pA cassette was transferred as a BsmBI fragment into the BsaI site flanked by two loxP sites, located 5' of the PGK-neo cassette in pBluescript. Finally,

the Vegfc-BGH-pA and PGK-neo cassettes were cloned as a NotI-AscI fragment into the p35ARM vector where the 5' and 3' homology arms had been inserted.

The targeting vector was electroporated into R1 (129/Sv × 129/SvJ) embryonic stem (ES) cells. Successfully targeted ES cell clones were screened by using genomic PCR and confirmed by Southern blotting. A positive ES cell clone was injected into blastocyst stage C57Bl/6 embryos to produce chimeric mice. Heterozygous mice were obtained and mated with the Flp deletor mouse strain to remove the Neo cassette, and the gene-targeted targeted mice subsequently mated to homozygosity. The homozygous *Vegfc*$^{flox/flox}$ mice were viable with no apparent phenotype. Mice with the *Vegfc*$^{flox/flox}$ and *Rosa26-CreER*^{T2} alleles (4) efficiently deleted of the *Vegfc* cDNA after 4-OHT treatment. The deletion induced swelling and death of embryos before E17.5 (n>4 embryos), as expected, based on our previous data on the constitutive *Vegfc* knockout mice (3).

Southern blotting

ES cell clones were screened by PCR across the 3' arm, and positive clones were confirmed by Southern blotting using external 3' and 5' probes. For the preparation of nonradioactive digoxigenin-labeled 5' and 3' external hybridization probes for *Vegfc* Southern blot analysis, we cloned a 598 bp sv129 mouse genomic DNA insert into the pCRII-TOPO vector by using PCR and primers (forward: 5'-CCC TTA AGA ATC CTT TGT TCA TTC TGG-3'; reverse: 5'-TGG ATA AAG ACA ACT GTA AGC CAA AAT ATG-3') and a 286 bp DNA insert using primers (forward: 5'-AAA TGA GGA AAA TTC CTA ATT AAA ATA TTA TAA AAA AAG-3'; reverse: 5'-AAG CTT GTT CGT GCA TTT TAT TAT TTA GG-3'). The resulting plasmids were EcoRI digested, gel purified and PCR digoxigenin-dUTP labeled (PCR DIG Probe Synthesis kit, Roche) using the above-

mentioned PCR primer pairs. Genomic DNA from WT and targeted ES cell clones (10 µg) was SpeI digested, electrophoresed in a 0.8% (w/v) Tris-Acetate-EDTA agarose gel, transferred overnight to a nylon membrane and fixed by UV cross-linking. Hybridization was performed using the DIG Easy Hyb hybridization reagent (Roche) and employing standard procedures for non-radioactive nucleic acid probes. Chemiluminescent detection was performed using the anti-Digoxigenin-AP Fab fragments (Roche) and the CDP-Star reagent (New England BioLabs). The expected molecular sizes of the digested fragments detected using the 5' probe are 15.3 kb for wild-type and 8.9 kb for the targeted allele, and using the 3' probe, 15.3 kb for wild-type and 9.6 kb for the targeted allele.

Real-time quantitative PCR

Total RNA was extracted and isolated from mouse lung samples using the NucleoSpin® RNA II Kit (Macherey-Nagel) according to the manufacturer's protocol. To eliminate contaminating DNA, RNase-free DNase I (lyophilized) was used during RNA isolation. Samples were quality-controlled using a Nanodrop ND-1000 or BioSpec-nano spectrophotometer. Reverse transcription into cDNA was performed with 1 µg of total RNA using iScript™ cDNA Synthesis Kit (Bio-Rad). Real-time quantitative PCR (RT-qPCR) was performed using TaqMan Gene Expression Assays (Applied Biosystems) and the iQ™ Supermix kit (Bio-Rad). RT-qPCR was carried out using a BIO-RAD C1000 Thermal cycler according to a standardized protocol. The TaqMan Gene Expression Assays used for mouse mRNA were Vegfc (Mm00437310_m1) and Gapdh (4352932E). The data were normalized to the endogenous control Gapdh to compensate for experimental variations. Fold changes were calculated using the comparative CT method.

PCR genotyping of the floxed Vegfc allele

Pups were genotyped by PCR with primers 5′-GTG ACT GGG CTT AAC CAC CCC A-3′ (forward), 5′- CCC GTC GGG CTC CGC TTC-3′ (reverse for Vegfc cDNA) and 5′-GTC CAG GAC TTG GGA GCC TCG GAT C-3′ (reverse for the first intron of Vegfc).

Lectin perfusion

Newborn pups were anesthetized with 180 mg/kg of ketamine and 18 mg/kg of zylazine. After performing a thoracotomy, 5 µl of fluorescein labeled *Lycopersicon Esculentum* (Tomato) Lectin (2 mg/ml) (Catalog No. FL-1171, Vector Laboratories) was injected into the left ventricle of the beating heart. After waiting 5 minutes, the mice were terminated and eyes were collected and fixed in 4% paraformaldehyde o/n in 4°C overnight for staining.

Tyramide signal amplification immunohistochemistry

For the tyramide signal amplification immunohistochemistry (TSA-IHC) staining of human paraffin embedded eyes, section were first deparaffinated in a decreasing alcohol series (xylene, absolute ethanol, 95%, 70%, 50%, H_20) and subjected to antigen retrieval with incubation in high pH buffer (10 mM Tris, 1mM EDTA, 0,05% Tween-20, pH 9,0) in the microwave for 15 minutes. After washes in PBS, endogenous peroxidase activity was quenched with incubation in 3% H_2O_2-MetOH (225 ml MetOH, 25 ml H_2O_2). After washes in H_2O, the slides were mounted onto racks with PBS, blocked with TNB for 30 minutes and primary antibodies were incubated in TNB overnight in +4C. On the second day, after washes with TNT, the appropriate biotinylated secondary antibody in TNB was incubated for 30 minutes. After washes with TNT, Streptavidin-HRP (NEL700001KT,

TSA kit, Perkin Elmer) was applied for 30 minutes. After washes, Biotin Tyramide Working Solution (NEL700001KT, TSA kit, Perkin Elmer) was applied for 10 min. at RT. After washes with TNT, Streptavidin-HRP (NEL700001KT, TSA kit, Perkin Elmer) was incubated for 30 minutes. After washed in TNT, slides were taken out of racks and treated with AEC (235 ml NaAc + 15 ml AEC + 250µl H_2O_2) for 10 min. After washes with PBS and rinsing with H_20, counterstaining with hematoxylin was applied and the slides were rinsed with running water and mounted with Aqua-Mount (Thermo Scientific).

Supplemental References

1. Joukov V et al. Proteolytic processing regulates receptor specificity and activity of VEGF-C. *EMBO J*. 1997;16(13):3898–3911.

2. Streilein JW. Ocular immune privilege: therapeutic opportunities from an experiment of nature. *Nat Rev Immunol*. 2003;3(11):879–889.

3. Karkkainen MJ et al. Vascular endothelial growth factor C is required for sprouting of the first lymphatic vessels from embryonic veins. *Nat Immunol*. 2004;5(1):74–80.

4. Vooijs M et al. A highly efficient ligand-regulated Cre recombinase mouse line shows that LoxP recombination is position dependent. *EMBO Rep*. 2001;2(4):292–297.